AIAA 81-0587R

Finite Element Modeling of the Hot Isostatic Pressuring Process

Brice N. Cassenti*
United Technologies Research Center, East Hartford, Conn.

In the hot isostatic pressing (HIP) process a container, with the approximate shape of the component to be produced, is filled with a metal powder, evacuated, and then subjected to high temperatures and pressures. As a result, the powder deforms to fill the void space and upon cooling a solid part results. Although the HIP process is cost competitive with forging, the costs for HIP could be reduced substantially if the final shape and size of the resulting component could be predicted. A computer aided modeling strategy for the HIP process has been developoed, and the results compare well with experimental measurements. This paper briefly discusses the macroscopic mechanical properties of powder metals, and the modifications of a finite element code required to include the powder mechanical properties. A more detailed discussion follows and includes: 1) the computer aided modeling strategy using a nonlinear finite element computer program, 2) the conclusions from a parametric study which indicated that the plastic deformations induced by the container were the primary source of the observed distortions, and 3) the results of a finite element model for an actual HIP which correlated well with experimental observations.

Introduction

THE technology for the fabrication of nickel base superalloy turbine engine components by powder metallurgy (PM) methods has advanced rapidly during the past decade. The strong emphasis on PM is the result of advanced engine technology requirements for higher performance alloys which are more difficult to process (cast, forge) and, hence, result in higher costs. Advanced PM technology for the production of near net shapes in superalloys offers the twofold advantage of producing complex engine components from the most advanced alloys without the need for either castability or workability in the alloy and doing so at significantly lower cost than current technology.

A substantial economic advantage for powder metallurgy materials can be achieved by direct hot isostatic pressing of components to near finished dimensions. The hot isostatic pressing (HIP) of components to near finished dimensions would minimize the cost of machining and save critical materials. The concept of HIP complex near-net shapes is simple. As is shown schematically in Fig. 1, a mold having the required configuration is filled with powder. The mold or container is out-gassed, sealed, placed in a HIP facility, raised to a temperature of over 1100°C and subjected to an external gas pressure of approximately 100 MN/m^2 (15 ksi).

During the HIP process the volume occupied by the powder decreases by 30-35%. The rate of powder compaction occurs as a result of surface tension forces and plastic deformation and is a function of temperature and pressure. Ideally this shrinkage is isotropic, so that the final shape is a uniformly reduced replica of the initial container shape. In practice, the final shape can depart substantially from that ideal shape depending on the techniques practiced. Because of this distortion and a current absence of systematically derived analytical tools to predict it, the full benefit of the HIP process has not been realized.

Presented as Paper 81-0587 at the AIAA/ASME/ASCE/AHS 22nd Structures, Structural Mechanics and Materials Conference, Atlanta, Ga., April 6-8, 1981; submitted April 24, 1981; revision received Aug. 24, 1981.

*Analytical Engineer. Member AIAA.

The principal objective was to develop a finite element methodology for predicting final size and shape of hot isostatically pressed axisymmetric powder metal structures. A constitutive model for the compaction of metal powders during the HIP process was constructed and an experimental program was executed to provide data for this model. An existing nonlinear finite element code which models both container and powder deformations during the HIP operation has also been modified. The modified code was then used to 1) determine the significant variables during numerical simulation of the HIP process through a parametric study and 2) model the HIP of a disk for which experimental observations existed.

The paper is divided into four parts: 1) a summary of the powder metal mechanical properties, 2) a brief description of the code modifications, 3) a summary of the results of the parametric study, and 4) a description of the numerical simulation of the HIP of a compressor disk. A more detailed discussion of each of the aforementioned topics can be found in Refs. 1 and 2.

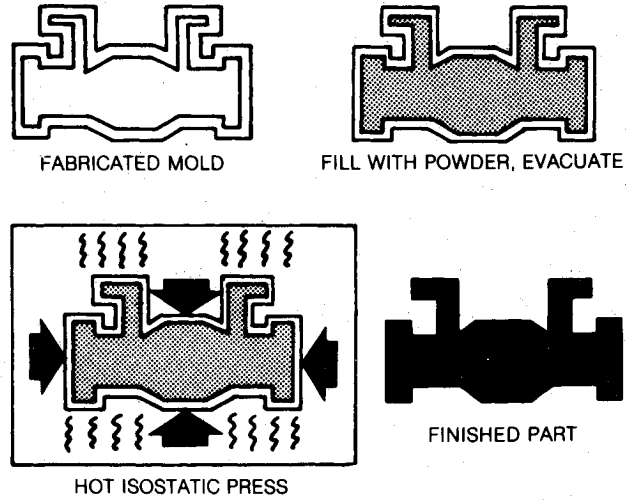

Fig. 1 Schematic of HIP process.

Powder Metal Mechanical Properties

The HIP process performs two functions: 1) densification of the loose powder metal aggregate and 2) endowment of the densified powder with mechanical strength. The process by which this occurs can be described microstructurally as passing through the several stages[3-5]: 1) particle rearrangement, fragmentation and plastic flow; 2) formation of isolated pores; 3) sphericalization of the isolated pores; and 4) closure of the spherical pores.

The driving forces for these stages are the applied external HIP pressure and particle surface free energy of which the former is typically much larger. Although the mechanisms which are active during these stages of the process are not fully understood, it is generally accepted that the principle mechanisms are plastic deformation, volume diffusion or Nabarro-Herring creep, grain boundary diffusion or Coble creep, and power law or dislocation creep.

Two approaches to modeling powder deformation and strength growth in the HIP process are possible. The first is based on continuum mechanics principles wherein microstructural effects are averaged over the powder aggregate. The second approach is to consider microstructural processes explicitly. Since the objective of this program is to predict overall powder response in the HIP process, the latter approach is not sufficient by itself. Rather, it may be used to aid development of continuum constitutive models by supplementing experimental work.[6]

The development of continuum constitutive models requires consideration of large strain effects since the initial void fraction is approximately 30%. This in turn implies a 30% volume reduction is necessary to obtain full powder densification. Both time-independent and time-dependent models must be considered, though time-independent plasticity effects can be expected to dominate. A finite strain plasticity theory requires: 1) specification of a yield surface to delineate regions of elastic and plastic response, 2) a hardening rule for the expansion of this yield surface, and 3) a flow rule for relating stress and strain increments. This flow rule must be formulated using large strain, stress, and strain rate measures.[7] Time effects require the specification of a creep law.

Classical plasticity and creep theories assume that materials undergoing permanent deformations do not sustain any change in volume, but in the HIP process the major portion of the deformation is a permanent volume change. Classical plasticity theory was modified to include this effect by assuming a yield surface quadratic in hydrostatic stress (i.e., the first invariant of the stress tensor) and Mises stress (i.e., the second invariant of the deviatoric stress tensor). The yield surface parameters were assumed to depend on void volume fraction and plastic work performed, and an associated flow rule was assumed for the plastic strains. From the preceding assumptions the plastic material moduli were developed, including the effects of large strains.

The creep deformations were assumed to consist of two parts, a volumetric creep and a deviatoric, or volume preserving, creep. In each of these two parts the creep strains were assumed to follow a steady-state power law creep model.

An experimental program was conducted to find the parameters in the plasticity and creep theories including the elastic parameters, and an independent experiment was performed to verify the plasticity theory developed.

In this paper the details of the plasticity theory development and the verification experiment will not be discussed. An analytical summary of the results, though, appears in the Appendix. A complete description of the plasticity theory and verification experiment can be found in Ref. 1.

Code Modifications

To analyze the powder plastic flow, the plasticity theory was incorporated into the MARC (MARC Analysis Research Corporation) finite element computer code. The MARC code

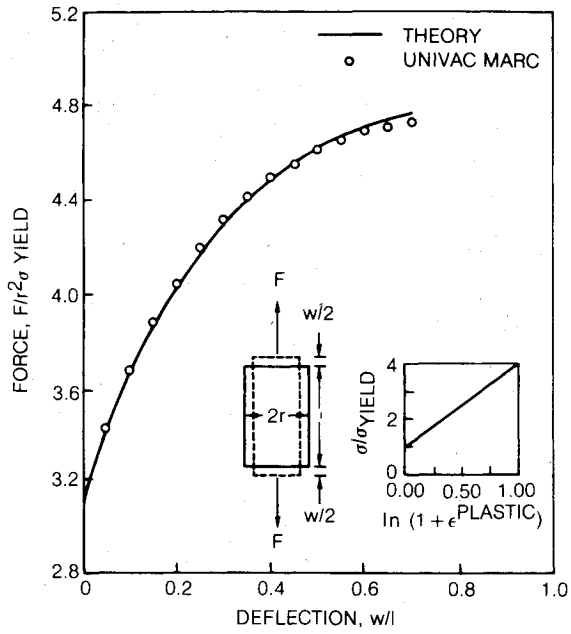

Fig. 2 Axisymmetric large strain test case.

applies the algorithm of Rice and Tracey,[8] in the subroutine THRUS. Therefore, one approach would be to modify THRUS to include nonvolume preserving plasticity. The MARC program also contains user subroutines which the general user writes to incorporate special features of his analytical model. One of these user subroutines, HYPELA, can be used for hypoelastic material properties (i.e., nonlinear elastic material properties). Subroutine HYPELA must output the final stress state and has for input an estimate of the strain increment, and the stress state from the previous increment. Subroutine HYPELA, therefore, is not limited to elastic response but is quite general. A third approach applying user subroutines appropriate to a specialized form of viscoplasticity can also be used.

Incorporating the nonvolume preserving plasticity theory into the MARC code through the user subroutine HYPELA requires writing only the one subroutine while modifications to THRUS would also require modifications to several connected subroutines. Therefore, the first step was to try HYPELA using the rigid plastic problem illustrated in Fig. 2. The test was successful with the numerical predictions nearly identical to the theoretical results. Therefore, the nonvolume preserving plastic flow equations were incorporated as modifications to the MARC code through the user subroutine HYPELA.

The first attempts at integrating the plastic flow equations were modifications of the algorithm developed by Rice and Tracey.[8] These attempts were only partially successful and a direct integration using Runge-Kutta was employed instead. Adapting a method described by Parks,[9] the Runge-Kutta integration strain increments are a fraction of the total strain step, where the fraction is specified by the user. If the final stress state drifts more than a user specified distance from the yield surface, the strain increments are reduced in size an amount again specified by the user. If the strain increments decrease below a user specified fraction of the total strain step, a correction to the final stress state is made by bringing the stress back to the yield surface along the normal to the yield surface, and the appropriate modification is made to the elastic-plastic moduli.

The MARC code modifications were run independent of the MARC code for several simple test cases, one of which is illustrated in Figs. 3 and 4. They show excellent agreement with the theoretical solution using approximately 1% total strain steps in the integration algorithm. In Figs. 3 and 4, the

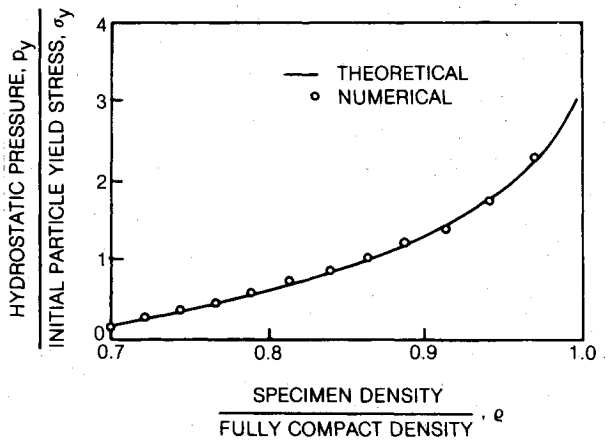

Fig. 3 Hydrostatic pressure test case results.

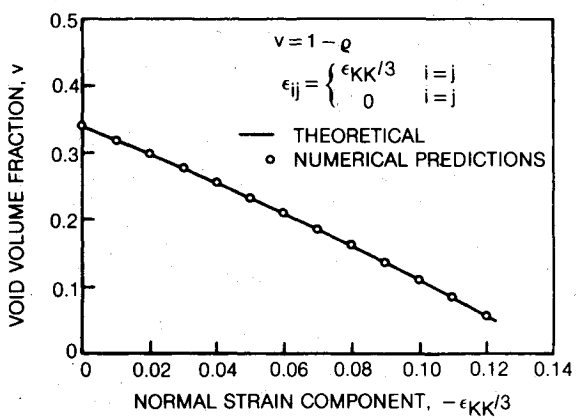

Fig. 4 Void volume fraction test case results.

material response when subjected to a uniform pressure is illustrated. Figure 3 presents the pressure as a function of the density and shows only minor variations between the numerical and theoretical response. The void volume fraction as a function of strain compares exactly as illustrated in Fig. 4. The stress state did vary from hydrostatic but the error in the second invariant of the deviatoric stress tensor was always less than 0.3×10^{-4} of the square of the initial powder particle yield stress, σ_y, in Eq. (A15). A uniaxial compression test case was exactly on the theoretical variation with the void volume fraction remaining constant to four places, a fact observed experimentally and included in the expressions in the Appendix. Both of the aforementioned cases were run with and without correcting the final stress state to bring the stress to the yield surface, with the same results to four significant figures.

The code modifications were then added to the MARC finite element code and tested on the same two sample cases. The agreement between the theoretical and the numerical code predictions was excellent although somewhat smaller strain steps (0.25-0.50%) were required for numerical stability. The unsymmetric part of the stiffness moduli was added to the MARC code and effects of creep were included either through the user subroutines CRPLAW and VSWELL or directly in the subroutine HYPELA.

Finite Element Modeling

The formulation of a finite element analysis requires the specification of a finite element mesh, material properties, external load histories, and boundary conditions. Additionally, since both material and geometric nonlinearities will be present, the finite element analysis must be incrementally loaded.

The geometry of a HIP configuration consists of a metal container which encapsulates a metal powder. For the applications considered in this paper the geometry will be axisymmetric. The container is modeled with axisymmetric thin shell elements and the powder with axisymmetric solid elements. The MARC code possesses both ring and shell elements. The axisymmetric ring elements are the three node triangular element and the four and eight node isoparametric quadrilateral elements. For the thin shell element model of the container a two node axisymmetric membrane and bending element is used. The axisymmetric solid elements can be generated using the MARC two-dimensional mesh generator. The thin shells must be generated manually.

The container elastic, plastic, and creep material properties are modeled using the finite-strain analogs of the classical, incompressible plasticity and creep theories. Thus the container material is characterized in terms of its uniaxial plastic and creep response at HIP temperatures. These data were developed separately and are described in Ref. 2.

In the HIP process three load types are present: gravity, the externally applied increasing pressure field, and temperature loads. All three loads should be modeled. Experimental evidence from the HIP of full scale disks has shown that gravitational loads produce gross distortion of the HIP containers not adequately supported around their base. The pressure load applied to the internal surface of the container is the principal driving force for powder consolidation. Finally, the effects of possible inhomogeneous temperature distributions must be considered since container and powder material properties are temperature dependent. Thus the effects of temperature gradients should be investigated.

Displacement boundary conditions must be specified to complete the definition of the HIP configuration to be modeled. The boundary conditions which model the HIP container support are simply no motion in the vertical direction at the container base. The evolving boundary conditions between the container and powder are not presently understood. Initially the powder is free to move relative to the container except on the container lower horizontal surfaces where the powder weight may be assumed to inhibit motion. As the temperature in the container and powder increases, differences in container and powder thermal expansion will result in either 1) a gap between the container sides and top, and the powder or 2) compressive stresses being exerted on the powder by the container. Irrespective of which of these conditions holds, it has been experimentally observed that at the end of the HIP process the container and powder are fused together. If there is an initial gap between the powder and container, the interior surfaces of the container walls and top are initially unsupported. The pressure loads are carried by the container alone causing the container walls to deform before contacting the powder. This nonuniform deformation in the container could contribute to nonuniformities in the final HIP geometry. Thus it may be necessary to model the closing of any gaps between the powder and container using the gap element technology in the MARC code. If the container is always in contact with the powder, an approximation to the container-powder interface would be complete bonding for the entire HIP cycle. Such an approximation can be implemented by the specification of multipoint constraints. In the analyses to follow, it will be assumed that no gaps have formed.

After the input data for the HIP analysis were assembled, an incremental load analysis was performed. Thus, increment sizes and increment convergence criteria were established. Increment size is controlled by the rate at which changes in material properties and geometry occur. Typically material properties change faster than the geometry so that it should not be necessary to account for geometry changes at every increment. At present, however, the MARC code does not allow for changing the frequency with which the geometry is updated. A future enhancement to accomplish this would be beneficial.

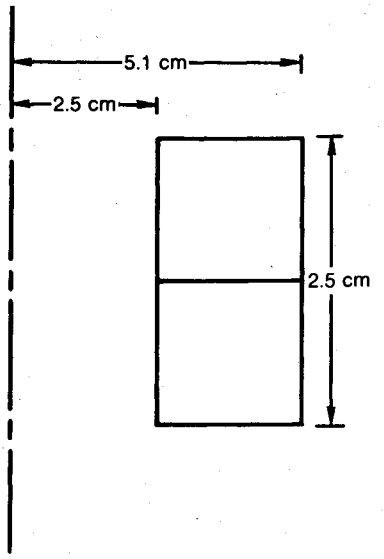

Fig. 5 Parametric study finite element model.

Parametric Study

An examination of the sensitivity of HIP finite element analysis can now be discussed. Parameters which were examined included: powder creep deformations, the assumption that large strains are important, temperature gradients in the powder, the effects of weight, and increment size and convergence criteria.

The two element parametric model, Fig. 5, was used to determine an efficient modeling strategy. The basic case consisted of a pressure loading only and produced a photographic reduction (i.e., a proportional change in all the dimensions). A 28°C linear temperature difference was applied with the top of the model 14°C higher than the mean of 982°C and the bottom 14°C lower. There was no radial variation. At 103 MN/m^2 (15 ksi) the bottom had a permanent radial displacement of 0.483 cm inward while the top moved 0.648 cm inward. This is a significant variation over a diameter of 10 cm. Instrumentation can produce errors in temperature of this order and therefore the temperature distribution should be accurately controlled and modeled. The unsymmetric part of the stiffness moduli was then added to the case with a temperature variation and the displacement predictions changed by less than 0.5%. This was found to be generally true and it appears that this effect can be neglected. Although the model used should be relatively insensitive to the effects of weight, the addition of gravitational forces did produce a slight additional permanent radial displacement at the bottom, and further study with more sensitive structures should be considered. When the large strain terms in the numerical analysis were deleted, inaccurate results were produced; the permanent radial displacements were overpredicted by 6%, a large error for an actual disk even though the modeled structure is relatively simple. Last, the effects of creep were added and a 1170°C the creep rate was high enough for the displacements to increase by 3.8×10^{-6} cm in 3 s due to the weight alone, and, therefore, during an actual HIP, the effects of creep should be included in the analyses. Simple analytical models for the effects of work hardening showed the effect to be slight, and, therefore, work hardening has not been examined numerically.

Disk HIP Analysis

To analyze an actual disk HIP two models were developed: 1) a 65-element model of the F100 11th stage compressor disk with 44 container shell elements and 21 quadrilateral elements to represent the powder, Fig. 6, and 2) a model of the inside

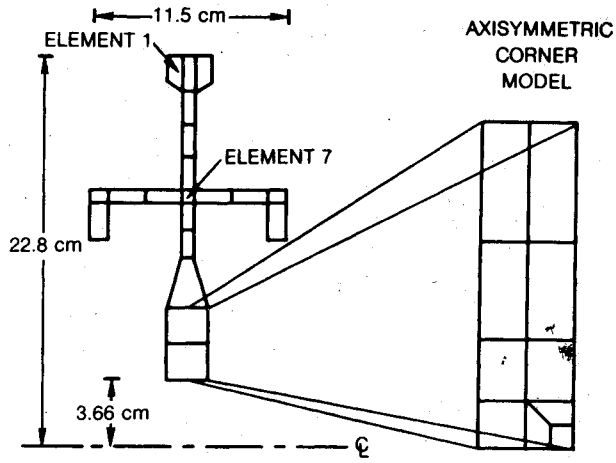

Fig. 6 Disk and corner finite element models.

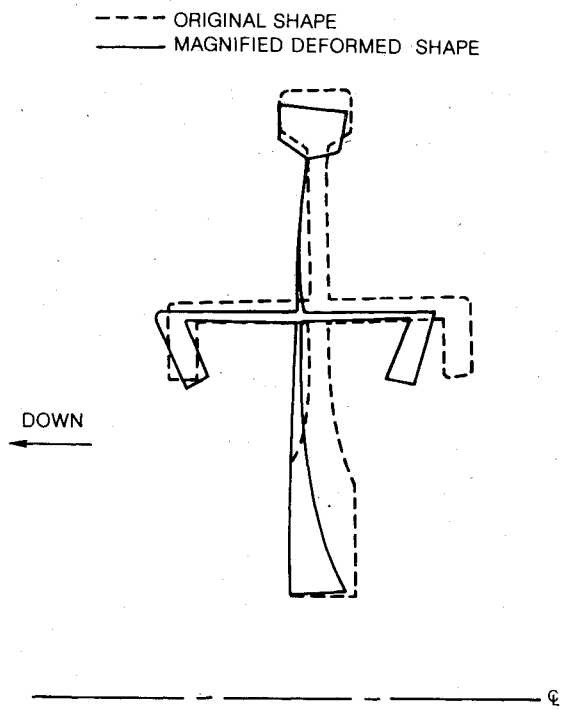

Fig. 7 Deformed shape of compressor disk.

corner of the F100 disk with 10 quadrilateral elements and 14 shell elements to study the distortions at corners, Fig. 6.

The axisymmetric shell elements chosen to represent the container in the disk and corner models did not represent accurately the effects of large strains. However, these elements were able to bring the analysis to about half the initial void volume fraction. Currently there are no operational shell elements in the MARC code capable of modeling the HIP process.

The corner model of Fig. 6 showed that the displacements are considerably different for the finer mesh than the coarse model of the entire disk. The corner model had an initial void volume fraction of 0.340 upon termination of the analysis the void volume fraction varied from 0.009 far from the corner to 0.238 for the element in the corner. A significant variation that would not be predicted by the full disk model.

The full disk analysis began with the powder having an initial density of 0.660 and upon termination of the analysis the central element in Fig. 6 had a void volume fraction of 0.194, while an outer element had a void volume fraction of 0.315. In Fig, 7, the displaced shape, with the displacements amplified, readily shows the effects of weight loading. The

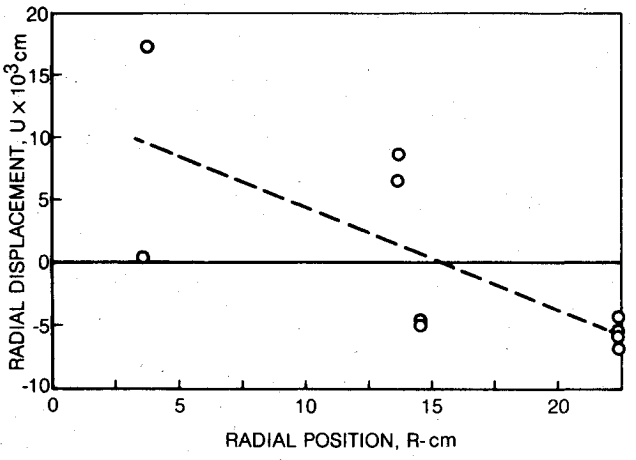

Fig. 8 Radial displacement on axial surfaces.

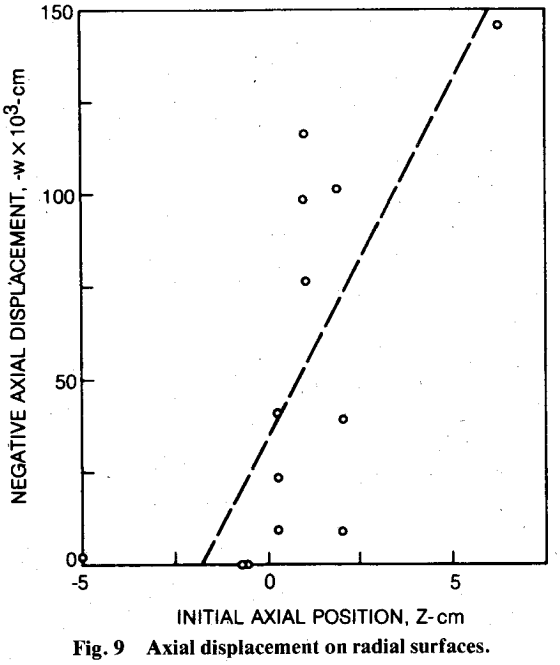

Fig. 9 Axial displacement on radial surfaces.

displacements predicted were used to derive general expresions for the final positions (r,z) in terms of the initial positions (R,Z). From the results of the analysis the initial and final positions were related approximately by

$$r=0.9919R+0.0129 \tag{1}$$

and

$$z=0.9798Z+0.0366 \tag{2}$$

which are derived by a least squares fit (see Figs. 8 and 9). Equation (1), from the finite element results, predicts a growing of the radius of the inside hole and a shrinking of the outer radii, which was experimentally observed. Equations (1) and (2) predict contractions that are larger axially than radially, which was also observed. At the point where the analysis was terminated the difference in contraction ratios (i.e., one minus either of the coefficients of R or Z) divided by the axial contraction ratio 0.599 compares well with the experimental value 0.648 obtained.[2] All of these facts indicate that the analysis is proceeding correctly and that an accurate model of the HIP powder response can be generated.

Conclusions

A computer-aided design procedure for analyzing the final shape of components produced by the hot isostatic pressing (HIP) process is being developed. The procedure promises to reduce the cost to manufacture components by HIP by: 1) reducing the number of design iterations required and 2) reducing the manufacturing operations performed after HIP (for example, fine machining and tuning). The results of a parametric study indicated that the major contribution to the distortions was the varying plastic response of the powder. The variation was due to the nonuniform pressure transmitted by the container which in turn was produced by the variations in container stiffness, especially at corners. An analysis of the HIP of a full disk indicated that the analysis procedure can predict observations made from an actual HIP.

Appendix: Summary of Power Mechanical Properties

The small strain mechanical response of a powder metal is decomposed according to

$$\dot{\epsilon}_{ij}=\dot{\epsilon}^e_{ij}+\dot{\epsilon}^p_{ij}+\dot{\epsilon}^c_{ij} \tag{A1}$$

where $\dot{\epsilon}_{ij}$ is the total strain rate, $\dot{\epsilon}^e_{ij}$ the elastic strain rate, $\dot{\epsilon}^p_{ij}$ the plastic strain rate, and $\dot{\epsilon}^c_{ij}$ the creep strain rate. For an isotropic material the elastic strain is given by

$$\dot{\epsilon}^e_{ij}=(1/E)[(1+\nu)\dot{\sigma}_{ij}-\nu\dot{\sigma}_{kk}\delta_{ij}] \tag{A2}$$

where $\dot{\sigma}_{ij}$ is the stress rate, δ_{ij} the Kronecker delta symbol, E Young's modulus, and ν Poisson's ratio. The elastic constants were determined experimentally[1] to be given by

$$E=E_1\exp\left[-\frac{T-T_0}{T_1}\right]\left(\frac{v_i-v}{v_i}\right) \tag{A3}$$

where E_1, T_0 and T_1 are material constants, T the temperature, v the void volume fraction, and v_i the initial void volume fraction. Poisson's ratio was taken to be given by[1]

$$\nu=\frac{1}{2}\left\{1-\frac{E_1}{3K_0}\exp\left[-\frac{T-T_0}{T_1}\right]\right\} \tag{A4}$$

where K_0 is a material constant.

The plastic strain rate was assumed to be governed by a yield surface of the form[1]

$$f(\sigma_{ij})=\beta^2\left(\frac{I_1+\alpha}{3}\right)^2+J_2-\sigma_0^2/3 \tag{A5}$$

and

$f(\sigma_{ij})<0$ when there is no plastic deformation

$f(\sigma_{ij})=0$ during plastic deformation

In Eq. (A5) I_1 is the first stress invariant or three times the mean Cauchy stress $\sigma_{kk}/3$, which is the hydrostatic pressure. Also,

$$J_2=\tfrac{1}{2}S_{ij}S_{ij} \tag{A6}$$

is the second variant of the deviatoric stress S_{ij} defined by

$$S_{ij}=\sigma_{ij}-I_1\delta_{ij}/3 \tag{A7}$$

Note that when β is zero Eq. (A5) reduces to the usual yield surface definition of metal plasticity

$$J_2-\sigma_0^2/3=0 \tag{A8}$$

Equation (A5) is an ellipse in $I_1, \sqrt{J_2}$ space with deformation dependent parameters $h_\alpha(\eta_\beta)$ where

$$h_1=\sigma_0(v,W^p) \qquad h_2=\beta(v,W^p) \qquad h_3=\alpha(v,W^p)$$

and

$\eta_1=v$ is the void volume fraction

$\eta_2=W^p=\int\sigma_{ij}\dot{\epsilon}^p_{ij}dt$ is the plastic work performed

The deformation parameters η_β are used to represent the hardening, or growth, of the yield surface.

Mechanical testing of partially dense hot isostatic pressed specimens indicated that there is little or no volume change in uniaxial compression. Coupling this fact with the hydrostatic pressure yield stress P_y, which is equal to the pressure at which the partially dense samples were hot isostatic pressed, and the compressive yield stress σ_c determines the three parameters in Eq. (A5) as

$$\alpha=\sigma_c \tag{A9}$$

$$\beta^2=3/q^2 \tag{A10}$$

$$\sigma_0=\sigma_c \tag{A11}$$

$$q=(3P_y/\sigma_c)-1 \tag{A12}$$

the hydrostatic yield pressure is described by[6]

$$\frac{P_y}{\sigma_y}=\frac{2}{3}\left[-\ell n\left(\frac{v}{v_i}\right)-\left(1-\frac{v}{v_i}\right)^2\ell n v_i+a\left(\frac{v}{v_i}\right)\left(1-\frac{v}{v_i}\right)\right] \tag{A13}$$

where v_i is the initial void volume fraction

$$a=\frac{Cv_i}{(1-v_i)\tan^2\theta}-1, \quad \cos\theta=\frac{\rho_i}{4}+\sqrt{\left(\frac{\rho_i}{2}\right)\left(\frac{1+\rho_i}{8}\right)} \tag{A14}$$

ρ_i is the initial relative density, and equal to $1-v_i$, and

$$C\approx 2.75 \tag{A15}$$

The temperature T and strain rate $\dot{\epsilon}$ dependence have been included in the initial particle yield stress σ_y

$$\sigma_y=\sigma_{y_0}\exp\left[-\frac{T}{T_0}\right]\left[1+\alpha_1\ell n\left(\frac{\dot{\epsilon}}{\dot{\epsilon}_0}\right)\right] \tag{A16}$$

σ_{y_0}, T_0, and α_1 are material constants and $\dot{\epsilon}_0$ can be chosen arbitrarily. The uniaxial compressive yield stress was taken to be given by[1]

$$\sigma_c=b\left(\frac{v-v_i}{1-v_i}\right)\sigma_y\{1-a_1\exp[-a_2W^p]\} \tag{A17}$$

where a_1 is a material constant

$$b=C/\tan^2\theta \tag{A18}$$

The constant a_2 was found to vary with temperature approximately by the relation[1]

$$\frac{1}{a_2}=\alpha_2\left(\frac{T_c-T}{\Delta T_0}\right) \qquad T\le T_c$$

$$=0 \qquad T\ge T_c \tag{A19}$$

The plastic strain rate was assumed to be given by an associated flow rule

$$\dot{\epsilon}^p_{ij}=\dot{\lambda}\frac{\partial f}{\partial\sigma_{ij}} \tag{A20}$$

where[1]

$$\dot{\lambda}=-\left[\dot{\sigma}_{ij}\frac{\partial f}{\partial\sigma_{ij}}\right]\Big/\left[k_\beta\left(\frac{\partial f}{\partial h_\alpha}\right)\left(\frac{\partial h_\alpha}{\partial\eta_\beta}\right)\right] \tag{A21}$$

$$k_1=2(1-v)\beta^2\left(\frac{I_1+\alpha}{3}\right) \tag{A22}$$

$$k_2=\frac{2}{3}\left[\sigma_0^2-\alpha\beta^2\left(\frac{I_1+\alpha}{3}\right)\right] \tag{A23}$$

The creep strain rates were decomposed into a volumetric creep rate ϵ^v_{ij} and a deviatoric or volume preserving creep rate ϵ^c_{ij}. The volumetric creep was assumed to be given by expressions first postulated by Wilkinson and Ashby[10]

$$\dot{\epsilon}^v_{ij}=-(\dot{\rho}/\rho)\delta_{ij} \tag{A24}$$

$$\dot{\rho}=k\left\{\frac{1}{t_0}\exp\left[-\frac{T_0}{T}\right]\right\}\frac{k}{N}\left(\frac{P}{\sigma_0}\right)^N\left\{\frac{\rho(1-\rho)}{[1-(1-\rho)^{1/N}]^N}\right\} \tag{A25}$$

where $3/2\le k\le 2$.

N, t_0, T_0 are material constants, and σ_0 can be chosen arbitrarily. The derivatoric creep was chosen to be governed by[1]

$$\dot{\epsilon}^c_{ij}=\Lambda S_{ij} \tag{A26}$$

where

$$\Lambda=\frac{3}{2}\frac{\dot{\bar{\epsilon}}^c}{\bar{\sigma}} \tag{A27}$$

$$\dot{\bar{\epsilon}}^c=\sqrt{2/3\dot{\epsilon}^c_{ij}\dot{\epsilon}^c_{ij}} \tag{A28}$$

is the equivalent deviatoric creep strain rate, and

$$\bar{\sigma}=\sqrt{3/2S_{ij}S_{ij}} \tag{A29}$$

is the Mises stress.

A power law creep function is assumed, or

$$\dot{\bar{\epsilon}}^c=(1/t_0)(\bar{\sigma}/\sigma_0)^n \tag{A30}$$

where σ_0 can be chosen arbitrarily and

$$t_0=a_0\exp[(T_0/T)+\gamma\rho] \tag{A31}$$

and

$$n=2-(v/v_i) \tag{A32}$$

the parameters a_0, T_0 and γ are material constants. A complete discussion of the mechanical properties, the evaluation of the material constants, and the results of mechanical testing can be found in Ref. 1.

Acknowledgments

The author would like to acknowledge Dr. David Parks for his help in developing the plasticity theory. The author would also like to thank Dr. Kenneth Cheverton for his aid in defining the early stages of the program. This research was sponsored by the Air Force Office of Scientific Research as a part of Contract F49620-78-C-0900.

References

[1]Cassenti, B. N., "Analytical Modeling of the Hot Isostatic Pressing Process," Air Force Office of Scientific Research, Washington, D.C., AFOSR TR-80-0592, July 1980.

[2]Cheverton, K. J., "Analysis of Container Shape Change During Hot Isostatic Pressing," United Technologies Research Center, E. Hartford, Conn., R79-217590, Sept. 1979.

[3]Wilkinson, D. S. and Ashby, M. F., "The Development of Pressure Sintering Maps," *Sintering and Catalysis Materials Science Research*, Vol. 10, Plenum Press, pp. 473-492.

[4]Notis, M. R., Smoak, R. H., and Krishnamacharin, V., "Interpretation of Hot Pressing Kinetics by Densification Mapping Techniques," *Sintering and Catalysis Materials Science Research*, Vol. 10, Plenum Press, pp. 493-507.

[5]Ramquist, L.,"Theories of Hot Pressing," *Powder Metallurgy*, Vol. 9, No. 17, 1966, pp. 1-25.

[6]Cassenti, B. N., "Manufacture of Disks by the Hot Isostatic Pressing Process," AIAA Paper 80-1111, July 1980.

[7]Nagtegaal, J. C. and deJong, J. E., "Some Computational Aspects of Elastic-Plastic Large Strain Analysis," MARC Analysis Research Corporation, Palo Alto, Calif., 1979.

[8]Rice, J. R. and Tracey, D. M., "Computational Fracture Mechanics," *Proceedings of the Symposium on Numerical and Computer Methods in Structural Mechanics*, Academic Press, New York, 1973, pp. 585-563.

[9]Parks, D., private communication, Massachusettes Institute of Technology, March 9, 1980.

[10]Wilkinson, D. S. and Ashby, M. F., "Pressure Sintering by Powder Law Creep," *Acta Metallurgica*, Vol. 23, Nov. 1975, pp. 1277-1285.